

An improved analytical model for the statistics of SET emergence point in HfO₂ memristive device

Cite as: AIP Advances **9**, 025118 (2019); <https://doi.org/10.1063/1.5085685>

Submitted: 13 December 2018 . Accepted: 14 February 2019 . Published Online: 22 February 2019

Dong Xiang, Rulin Zhang, Yu Li,  Cong Ye, Enrique Miranda,  Jordi Suñé, and Shbing Long



View Online



Export Citation



CrossMark

ARTICLES YOU MAY BE INTERESTED IN

Sub-nanosecond pulse programming and device design strategy for analog resistive switching in HfO_x-based resistive random access memory

Applied Physics Letters **114**, 112102 (2019); <https://doi.org/10.1063/1.5078782>

Perspective: A review on memristive hardware for neuromorphic computation

Journal of Applied Physics **124**, 151903 (2018); <https://doi.org/10.1063/1.5037835>

Comprehensive numerical modeling of filamentary RRAM devices including voltage ramp-rate and cycle-to-cycle variations

Journal of Applied Physics **124**, 174502 (2018); <https://doi.org/10.1063/1.5042789>

Call For Papers!

AIP Advances

**SPECIAL TOPIC: Advances in
Low Dimensional and 2D Materials**



An improved analytical model for the statistics of SET emergence point in HfO_2 memristive device

Cite as: AIP Advances 9, 025118 (2019); doi: 10.1063/1.5085685

Submitted: 13 December 2018 • Accepted: 14 February 2019 •

Published Online: 22 February 2019



View Online



Export Citation



CrossMark

Dong Xiang,¹ Rulin Zhang,² Yu Li,³ Cong Ye,^{2,a} Enrique Miranda,⁴ Jordi Suñé,⁴ and Shibing Long^{5,a}

AFFILIATIONS

¹ School of Mechatronics Engineering, Harbin Institute of Technology, Harbin 150001, China

² Hubei Key Laboratory of Applied Mathematics, Faculty of Physics and Electronic Science, Hubei University, Wuhan 430062, China

³ Key Laboratory of Microelectronics Devices & Integration Technology, Institute of Microelectronics of Chinese Academy of Sciences, Beijing 100029, China

⁴ Departament d'Enginyeria Electrònica, Universitat Autònoma de Barcelona, Bellaterra 08193, Spain

⁵ School of Microelectronics, University of Science and Technology of China, Hefei 230027, China

^a Corresponding authors: yecong@issp.ac.cn (Cong Ye); shibinglong@ustc.edu.cn (Shibing Long)

ABSTRACT

In this work, an improved analytical model for the SET switching statistics of HfO_2 memristive device is developed from the cell-based percolation model. The statistical results of the SET emergence point related to the beginning stage during SET process are systematically discussed. Moreover, the deviation from Weibull model in high percentiles region is found to originate from the uneven distribution of defect density. Our improved model exhibits excellent consistency with experimental results in $\text{Cu}/\text{HfO}_2/\text{Pt}$ device. Besides, we explain the relationship between the parameters of the model and SET resistance. The underlying mechanism of SET process for HfO_2 memristive device is fully illuminated.

© 2019 Author(s). All article content, except where otherwise noted, is licensed under a Creative Commons Attribution (CC BY) license (<http://creativecommons.org/licenses/by/4.0/>). <https://doi.org/10.1063/1.5085685>

Memristor, also called resistance switching device, is a two-terminal device whose resistance values can be modulated by the external stimulation, and has attracted extensive interest as promising candidates for non-volatile memories, reconfigurable switches, and bio-inspired neuromorphic computing.^{1–4} As a promising device applied in non-volatile memory field, memristor has shown highly desirable properties including low power, fast switching speed, excellent retention and scalability.² Especially, HfO_2 material, which is highly compatible with complementary metal oxide semiconductor (CMOS) technology, is applied in memristor, showing narrow resistance distributions, reliable endurance, and robust thermal stability.⁵ However, the wide fluctuation of resistive switching parameters is a major obstacle for practical application. The randomness is mainly induced by the uncontrolled formation and rupture of conductive filament

(CF) in the resistive switching (RS) layer. Moreover, the underlying mechanisms of SET/RESET switching processes have not been fully illuminated. Hence, understanding the RS mechanism is the key aspect to control the parameter randomness. By means of statistical analysis with Weibull model, the statistical distributions of resistive parameters can be investigated,⁶ which would help to reveal the undetected behavior of CF and disclose the RS mechanism.^{7–12}

We have investigated the dynamic CF evolution in SET process of memristive device.^{6,13,14} Different from the usually reported abrupt SET switching, some RRAM devices, for example, the $\text{Cu}/\text{HfO}_2/\text{Pt}$ device studied in this work, show complicated SET process with multiple steps. At a low voltage, the resistance keeps comparatively stable because the external electrical stimulations are not strong enough to induce the CF growth in the RS layer. With the increase of the applied volt-

age, the SET emergence point occurs, indicating the beginning of CF growth. The SET emergence point is a bridge between the initial high resistance state and the SET process, and it obviously affects the self-accelerating SET process. Generally, the CF shows obvious fluctuation at a high voltage and leads to a final abrupt formation of the connected CF, which is corresponding to the SET point. As the SET switching includes different stages similar to those in RESET switching,¹⁴ it's necessary to reveal the property of the SET emergence point through experiments especially the statistic ones and also deeply understand its physical mechanism. In our previous work, cell-based analytical percolation model to study the SET switching process has been built, and Weibull distributions of the SET parameters have been demonstrated on the basis of the Weibull model.^{6,13,14} However, if we apply the Weibull model to investigate the SET emergence point, the tail bits phenomenon are apt to appear in high percentiles region. Although it has been reported that the defects in RS layer are inclined to cluster when the defect density is high enough,¹⁵⁻¹⁹ the Weibull model cannot solve the tail bits phenomenon for SET process in high percentiles region. It is necessary to introduce a more exact or improved model to analyze the statistical experiment data, which can explore the inherent RS mechanism of HfO₂ memristive device more precisely.

In this work, as concerned as SET emergence point, an improved clustering statistic model with the influence of defect density is taken into account to analyze the statistical characteristic of the experimental data for Cu/HfO₂/Pt device. The relationship between SET resistance (R_{SET}) and RS parameters (Weibull slope, scale factor and clustering factor) is discussed to understand the underlying switching mechanism. The improved modeling method provide an excellent method for analyzing resistive parameters and the deviation in high percentiles region, which provides guidance for understanding the RS parameters fluctuation for HfO₂ memristive device.

In order to investigate the CF evolution and explain the statistical characteristics of RS parameters in SET process for Cu/HfO₂/Pt device, the cell-based model shown in Fig. 1(a) has been commonly proposed.⁸⁻¹⁰ The formation/rupture of CF mainly occurs in a small cell-described region, and the

dynamic evolution of CF can be regarded as the cell's evolution in the most constrictive part, i.e., the bottleneck region.²⁰ Here, we deduce that the bottleneck region contains a certain number of cells, which have the same switching probability irrespective of their spatial position. The cells are assumed to be divided into n slices, describing the length of the bottleneck region. Each slice contains N cells, which indicates the width of the region. According to the geometric model, the SET dynamic process for Cu/HfO₂/Pt device can be conveniently considered on the variation in those $n \times N$ cells. The thickness of every cell is a_0 . Moreover, it is supposed that these insulating cells share the same conductive probability λ_c . Importantly, the emergence point in SET process corresponding to the abrupt rise of current (Fig. 1(b)) is defined as the critical point, which indicates that at least one cell switches into conductive state. Thus, the SET emergence probability can be represented as

$$F_{SET} = 1 - (1 - \lambda_c)^{nN}, \quad (1)$$

Where F_{SET} is the cumulative probability. Therefore, Weibull distribution function $W = \ln[-\ln(1 - F)]$ can be replaced by

$$W_{SET} = \ln[-\ln(1 - \lambda_c)^{nN}], \quad (2)$$

In previous Weibull models, one tends to assume that defects are evenly distributed in the whole region with an average defect density (D_0) and the density function ($f(D)$) of uniform defect density (D) is a "delta" function $f(D) = \delta(D - D_0)$.¹⁰ According to the Poisson distribution function, the probability λ_c can be represented as

$$\lambda_c = 1 - \exp(-D_0), \quad (3)$$

In the general case of emergence point, conductive probability λ_c is comparatively low ($\lambda_c \ll 1$), thus the Weibull distribution function W_{SET} can be approximated expressed as follows:

$$W_{SET} \approx \ln(nND_0), \quad (4)$$

Furthermore, when we use Weibull distribution to describe the SET switching distribution, it can be defined as $W(x) = \beta \ln\left(\frac{x}{x_{63\%}}\right)$, so the Weibull distribution of V_{SET} and I_{SET} can also be innovatively expressed as:

$$W_{V_{SET}} = \beta_{V_{SET}} \ln\left(\frac{V_{SET}}{V_{SET,63\%}}\right), \quad (5)$$

$$W_{I_{SET}} = \beta_{I_{SET}} \ln\left(\frac{I_{SET}}{I_{SET,63\%}}\right), \quad (6)$$

where $\beta_{V_{SET}}$ (or $\beta_{I_{SET}}$) and $V_{SET,63\%}$ (or $I_{SET,63\%}$) are the Weibull slope and scale factor of V_{SET} (or I_{SET}) distribution, respectively. It is worth noting that these expressions for improved analytical model in HfO₂ memristive device have never been adopted to describe the statistics of SET emergence point previously.

On the basis of traditional Weibull model, we assume the defects are evenly distributed in the bottleneck region. However, when the sweep voltage is relatively high, the defects existing in the bottleneck region tend to cluster and the defect density increases, hence the distribution of defect density becomes uneven.^{17,19,21} As a result, the Gamma distribution

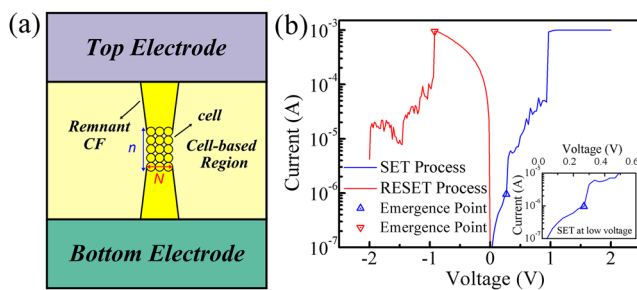


FIG. 1. (a) Schematic of $n \times N$ cells in the cell-based region. (b) $I-V$ characteristics of SET (blue line) and RESET (red line) in Cu/HfO₂/Pt device. The blue and red triangles indicate the emergence point of SET and RESET process, respectively. Inset of (b) shows the magnified plot of low voltage region in SET process.

is adopted to describe density function of defect instead of delta distribution. According to the Poisson-gamma mixture model,²² the probability λ'_c can be expressed as:

$$\lambda'_c = 1 - \left(1 + \frac{D_0}{\alpha_{\text{SET}}}\right)^{-\alpha_{\text{SET}}}, \quad (7)$$

where α_{SET} is represented as the clustering factor, reflecting the impact of uneven defect density on the SET process.¹⁶ At the same time, we should notice that when $\alpha_{\text{SET}} \rightarrow \infty$, Eq. (7) can be simplified to Eq. (3), which means the Poisson model has been changed to delta model and the defect in the bottleneck region becomes uniform distribution. When we substitute Eq. (7) into Eq. (2), we can get

$$W'_{\text{SET}} = \ln\left[-\ln(1 - \lambda'_c)^{nN}\right] = \ln\left[-\ln\left(1 + \frac{D_0}{\alpha_{\text{SET}}}\right)^{-nN\alpha_{\text{SET}}}\right], \quad (8)$$

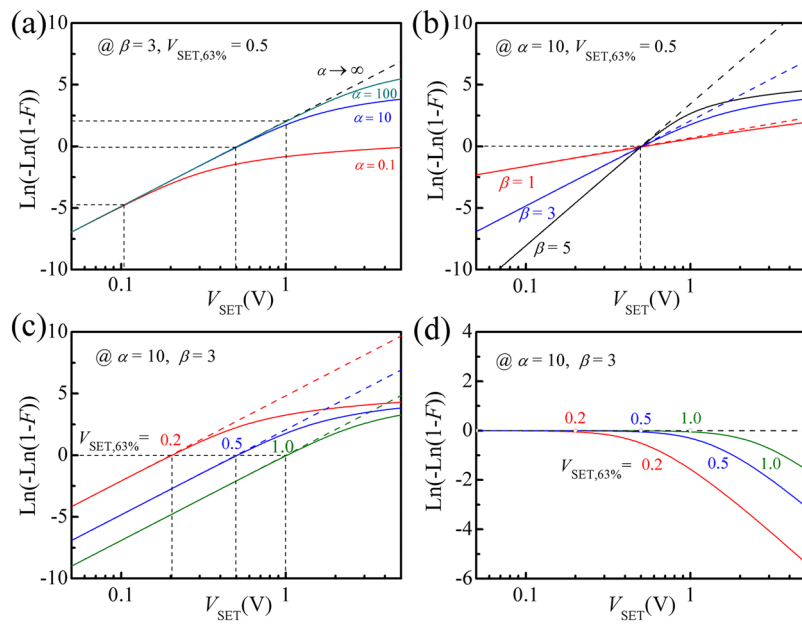
In RS layer, the defect density (D_0) is relatively low, thus, when $D_0 \ll 1$, Eq. (8) becomes

$$W'_{\text{SET}} = \ln(\alpha_{\text{SET}}) + \ln\left[\ln\left(1 + \frac{nND_0}{\alpha_{\text{SET}}}\right)\right]. \quad (9)$$

Eq. (9) expresses our improved clustering model with clustering factor (α_{SET}) for the SET emergence point statistics. By combining Eqs. (4), (5), (6) and (9), we can get the complete expression of the distribution of V_{SET} and I_{SET} :

$$W'_{V_{\text{SET}}} = \ln(\alpha_{V_{\text{SET}}}) + \ln\left[\ln\left(1 + \frac{1}{\alpha_{V_{\text{SET}}}} \left(\frac{V_{\text{SET}}}{V_{\text{SET},63\%}}\right)^{\beta_{V_{\text{SET}}}}\right)\right], \quad (10)$$

$$W'_{I_{\text{SET}}} = \ln(\alpha_{I_{\text{SET}}}) + \ln\left[\ln\left(1 + \frac{1}{\alpha_{I_{\text{SET}}}} \left(\frac{I_{\text{SET}}}{I_{\text{SET},63\%}}\right)^{\beta_{I_{\text{SET}}}}\right)\right], \quad (11)$$



On the basis of the above serials formula corrections and analysis, Fig. 2(a) displays the results of the Weibull model and the improved clustering model under different values of clustering factor α . It is worth noting that at low percentiles region with relatively low V_{SET} , Weibull model and clustering model have the same tendency and nearly overlap. The driven force of electric field is not strong enough to drive the defects to induce significant clustering effects,^{16,20} and the defects are still apt to have relatively uniform distribution upon the bottleneck region. As a result, when $\alpha_{\text{SET}} \rightarrow \infty$, the improved clustering model tends to coincide with the Weibull model, which means the clustering effect can be ignored. However, at high percentiles region with high V_{SET} , the deviation of both models can be clearly observed, which can be assumed to the clustering phenomenon of the defects. Fig. 2 (b) displays the results of the Weibull model and the improved clustering model under different values of Weibull slope β . The $V_{\text{SET},63\%} = 0.5$ means the separation point of both models. Especially, when the value of Weibull slope β changes, the cross point is fixed. Fig. 2(c) displays the Weibull model and clustering model under different values of scale factor $V_{\text{SET},63\%}$. It can be observed that the curves of both models are consistent in low percentiles region, but the curves of improved clustering model bend downward in high percentiles region. To explore the separation point of two models, the crossing point of fitting lines with $\ln(-\ln(1-F)) = 0$ can be defined as the separation of two models, which are displayed in Fig. 2(d). When the SET voltage is less than $V_{\text{SET},63\%}$, indicating that the distribution of defects is uniform, so it can be seen that the results extracted from Weibull model and clustering model show consistency well. When V_{SET} is higher than $V_{\text{SET},63\%}$, the defects emerge to cluster and the results of both models show much derivation, which suggest that the Weibull

FIG. 2. Plots of previous Weibull model(dashed lines) and our improved analytical model(solid lines) under different values of (a) clustering factor α , (b) Weibull slope β and (c) scale factor $V_{\text{SET},63\%}$. (d) Results extracted from improved analytical model and Weibull model. The intersection points indicate the value of $V_{\text{SET},63\%}$.

model needs to be improved and our analytical model is necessary.

Just as we have reported, the initial conductance strongly affects the current evolution in each SET cycle,²³ we use the SET resistance ($R_{SET} = V_{SET}/I_{SET}$) just at the SET emergence point, where a current jump can be observed (as shown in Fig. 1(a)) for the analysis of the V_{SET} statistics. Normally, R_{SET} is related to the CF size and morphology at the set emergence point. In order to explore the influence factor of the distribution parameters (Weibull slope, scale factor, clustering factor), we develop a deterministic model to relate the SET parameters' statistics with SET resistance. In the DC voltage sweeping mode (VSM), which is used for the practical measurement of the device,²⁴ a ramped voltage with $V(t) = \gamma t$ is applied. Considering the dynamic evolution of defects, the defect density D_0 can be described by the power law⁸

$$D_0 = \left\{ \int_0^{t_{SET}} \frac{1}{\tau_{T(t)}} dt \right\}^\rho, \quad (12)$$

where $\tau_{T(t)} = \tau_{TO} \left(\frac{V}{t_{gap}} \right)^{-m}$ is the characteristic time for defect generation⁸ with τ_{TO} and m being constants, and ρ is an exponent that provides flexibility to the model. According to our previous study,^{9,13} a tunnel gap (the bottleneck region which consist of $n \times N$ cells, as shown in Fig. 1(a)) associated with the first quantized subband forms at the constriction bottleneck. Here, we define its length as t_{gap} . According to the quantum point contact (QPC) model, which has been used to successfully describe the I-V curves of memristive device in both the LRS and HRS,^{25,26} we can get $t_{gap} = \frac{\hbar}{\pi} \sqrt{\frac{2}{m^* \phi_B}} \ln(G_0 N_{ch} R_{SET})$, where \hbar is the reduced Planck constant, m^* is the effective electron mass, ϕ_B is the height of the tunneling barrier in the conducting channels, $G_0 = 2e^2/h$ is the quantum of conductance, the reduced Planck constant and N_{ch} is the number of opened conducting channels.²⁷ By introducing the result of the QPC model, the physical nature such as effective electron mass, barrier height, etc, which has been deeply studied in previous work,²⁸⁻³⁰ is combined into our analytical model. Combining the above equation and Eqs. (12) and (9), the Weibull slope and scale factor of V_{SET} distribution can be expressed as:

$$\beta_{V_{SET}} = (m+1)\rho, \quad (13)$$

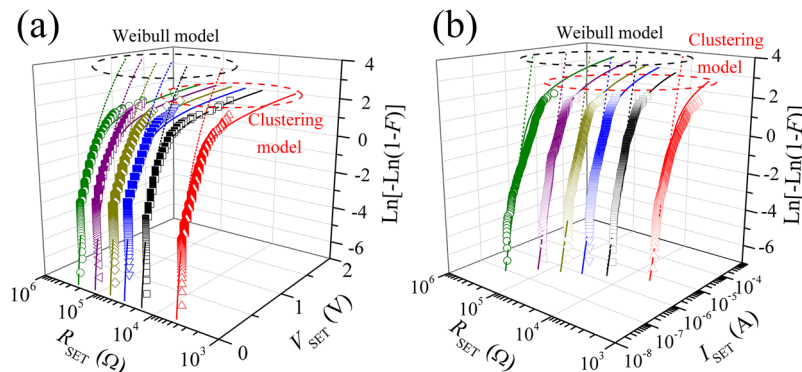


FIG. 3. Statistical results of (a) V_{SET} and (b) I_{SET} in 4000 cycles of Cu/HfO₂/Pt device.

$$V_{SET,63\%} = \frac{(\tau_{TO} \gamma^m (m+1))^{\frac{1}{m+1}} (t_{gap})^{\frac{m}{m+1}}}{(nN)^{\frac{1}{(m+1)\rho}}} \propto \ln(R_{SET}). \quad (14)$$

Using the same method, we can get:

$$\beta_{I_{SET}} = (m+1)\rho, \quad (15)$$

$$I_{SET,63\%} \propto \frac{1}{\ln(R_{SET})}. \quad (16)$$

In order to investigate the statistics of the SET emergence point, resistance screening method is adopted, so that the results would be expected to exhibit resistance-dependent characteristics. Figs. 3(a) and (b) show the distributions of V_{SET} and I_{SET} in 4000 cycles of Cu/HfO₂/Pt device. The dots, dotted lines and solid lines represent the experiment data, fitting results of Weibull model and improved clustering model, respectively. From Fig. 3, we can see both the fitting lines (dotted lines and solid lines) reveal good consistency with experimental data in low percentiles regions. However, as the SET voltage increases to high percentile regions, the Weibull model begins to separate from the experiment results while the improved clustering model still shows excellent consistency with the experiments. From our improved clustering model, this phenomenon can be explained as the influence of uneven defect density in high SET voltage region, as discussed above. If we use the Weibull distribution to describe the set emergence point of our experiment, we can observe the "tail bit" effect in high percentiles region.²² The reason lies in that the new generation of uneven defects would form clustering phenomena in high percentiles region and the traditional Weibull model deviates from the experiment.

Analogous to the method in Weibull model, values of three relevant parameters related to V_{SET} and I_{SET} distributions are extracted from experimental results, as shown in Fig. 4. It can be seen that when the R_{SET} increases, the Weibull slopes and clustering factors keep constant. However, the scale factors exhibit different dependence with the R_{SET} . It can be seen with the increase of R_{SET} , $V_{SET,63\%}$ increases while $I_{SET,63\%}$ decreases linearly. Actually, the clustering factor α is a constant independent of R_{SET} , which is related to the properties of materials and structure for the memristive device.^{24,31} Meanwhile, Eqs. (13) and (15) explain well that the Weibull slopes constant is independent on R_{SET} . Eqs. (14) and (16) show a

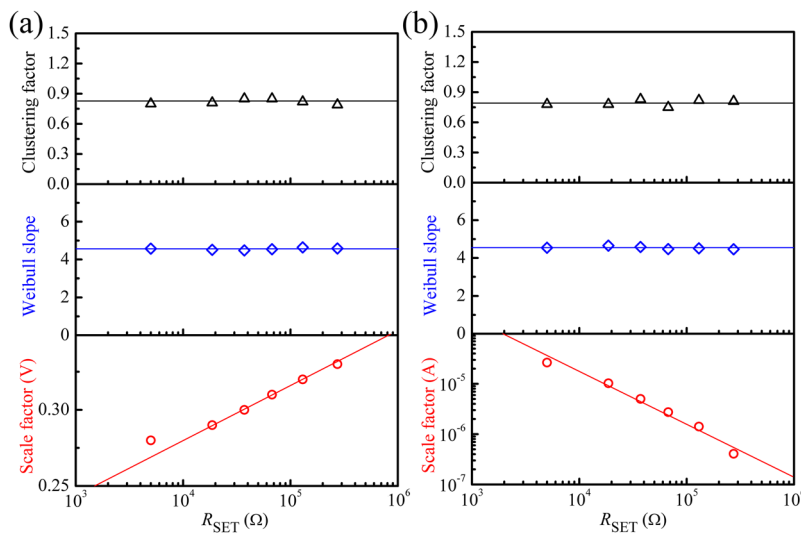


FIG. 4. Distribution parameters extracted from statistical results of (a) V_{SET} and (b) I_{SET} distributions.

clear relation between $I_{SET,63\%}$ (or $V_{SET,63\%}$) and R_{SET} , which agrees well with the experimental results shown in Fig. 4. Furthermore, we find that the parameter $V_{SET,63\%}$ (or $I_{SET,63\%}$) can be controlled by adjusting the value of R_{SET} , which provides guidance for understanding the switching mechanism and experimentally modulating the switching fluctuation.

In this work, an improved statistic model for the SET switching statistics of HfO_2 memristive device is developed for analyzing the emergence point in SET process. By adopting Gamma distribution function, the impact of uneven defects density is taken into consideration, and a new clustering factor is introduced to represent the influence of defects density. From the statistical results of emergence points, our improved model exhibits excellent consistency with the experimental results in SET process, and especially, the distribution of “tail bits” in high percentiles region can also be predicted. Therefore, this analytical model provides a reasonable explanation for the switching mechanism, and can be regarded as an effective method to evaluate performance behavior of CF dominated memristive device.

This work was supported by the National Natural Science Foundation of China (NSFC) (Grant No. 61774057), and the Opening Project of the Key Laboratory of Microelectronic Devices & Integration Technology, Institute of Microelectronics of Chinese Academy of Sciences (Grant No. Y7YS013001). National Key Research and Development Program under Grant 2017YFB0405600; The Open Fund of State Key Laboratory on Integrated Optoelectronics (IOSKL2018KF08). The Open Fund of Hubei Key Laboratory of Applied Mathematics (HBAM 201801).

REFERENCES

1. S. Schweiger, R. Pfenninger, W. J. Bowman, U. Aschauer, and J. L. Rupp, *Adv. Mater.* **29**, 1605049 (2017).
2. P. Chen, T. Chang, K. Chang, T. Tsai, C. Pan, and M. C. Chen, *ACS Appl. Mater. Inter.* **9**, 3149 (2017).
3. F. Pan, C. Chen, Z. S. Wang, and J. Yang, *Prog. Nat. Sci. Mater.* **20**, 1 (2010).
4. C. Ye, J. J. Wu, G. He, J. Zhang, T. F. Deng, P. He, and H. Wang, *J. Mater. Sci. Technol.* **32**, 1 (2016).
5. A. Padovani, J. Woo, H. Hwang, and L. Larcher, *IEEE Electron Device Lett.* **39**, 672 (2018).
6. S. Long, C. Cagli, D. Ielmini, M. Liu, and J. Suñé, *J. Appl. Phys.* **111**, 074508 (2012).
7. G. Bersuker, D. C. Gilmer, D. Veksler, P. Kirsch, L. Vandelli, A. Padovani, L. Larcher, K. McKenna, A. Shluger, V. Iglesias, M. Porti, and M. Nafria, *J. Appl. Phys.* **110**, 124518 (2011).
8. S. Long, X. Lian, C. Cagli, L. Perniola, E. Miranda, M. Liu, and J. Suñé, *IEEE Electron Device Lett.* **34**, 999 (2013).
9. M. Zhang, G. Wang, S. Long, Z. Yu, Y. Li, D. Xu, H. Lv, Q. Liu, and E. Miranda, *IEEE Electron Device Lett.* **36**, 1303 (2015).
10. S. Long, C. Cagli, D. Ielmini, M. Liu, and J. Suñé, *IEEE Electron Device Lett.* **32**, 1570 (2011).
11. S. Long, X. Lian, C. Cagli, L. Perniola, E. Miranda, D. Jiménez, H. Lv, Q. Liu, L. Li, and Z. Huo, *IEEE Int. Reliab. Phys. Symp. Proc.* **5A** (2013).
12. S. Long, X. Lian, T. Ye, C. Cagli, L. Perniola, E. Miranda, M. Liu, and J. Suñé, *IEEE Electron Device Lett.* **34**, 623 (2013).
13. M. Zhang, S. Long, G. Wang, X. Xu, Y. Li, Q. Liu, H. Lv, X. Lian, E. Miranda, and J. Suñé, *Appl. Phys. Lett.* **105**, 193501 (2014).
14. S. Long, L. Perniola, C. Cagli, J. Buckley, X. Lian, E. Miranda, F. Pan, M. Liu, and J. Suñé, *Sci. Rep.* **3**, 2929 (2013).
15. J. Suñé, *IEEE Electron Device Lett.* **22**, 296 (2001).
16. E. Y. Wu, B. Li, and J. H. Stathis, *Appl. Phys. Lett.* **103**, 152907 (2013).
17. K. Xiong, J. Robertson, M. C. Gibson, and S. J. Clark, *Appl. Phys. Lett.* **87**, 183505 (2005).
18. A. Kerber, E. Cartier, L. Pantisano, and R. Degraeve, *IEEE Electron Device Lett.* **24**, 87 (2003).
19. S. Zafar, A. Kumar, E. Gusev, and E. Cartier, *IEEE Trans. Device Mater. Reliab.* **5**, 45 (2005).
20. H. Sun, M. Zhang, Y. Li, S. Long, Q. Liu, H. Lv, J. Suñé, and M. Liu, *Appl. Phys. Lett.* **110**, 123503 (2017).
21. Y. Li, S. Long, Q. Liu, H. Lv, and M. Liu, *Small* **13**, 1604306 (2017).
22. S. Yu, X. Guan, and H. S. Wong, *IEEE Trans. Electron Devices* **59**, 1183 (2012).
23. Y. Li, M. Zhang, S. Long, J. Teng, Q. Liu, H. Lv, E. Miranda, J. Suñé, and M. Liu, *Sci. Rep.* **7**, 11204 (2017).

²⁴J. Suñé, S. Tous, and E. Y. Wu, *IEEE Electron Device Lett.* **30**, 1359 (2009).

²⁵E. A. Miranda, C. Walczyk, C. Wenger, and T. Schroeder, *IEEE Electron Device Lett.* **31**, 609 (2010).

²⁶X. Lian, X. Cartoixa, E. Miranda, L. Perniola, R. Rurrali, S. Long, M. Liu, and J. Suñé, *J. Appl. Phys.* **115**, 244507 (2014).

²⁷E. Miranda and J. Suñé, *IEEE Int. Reliab. Phys. Symp. Proc.* **39**, 367 (2002).

²⁸Z. Sun, Y. Zhao, M. He, L. Gu, C. Ma, K. Jin, D. Zhao, N. Luo, Q. Zhang, N. Wang, W. Duan, and C. Nan, *ACS Appl. Mater. Interfaces* **8**, 11583 (2016).

²⁹Y. Luo, D. Zhao, Y. Zhao, F. Chiang, P. Chen, M. Guo, N. Luo, X. Jiang, P. Miao, Y. Sun, A. Chen, Z. Lin, J. Li, W. Duan, J. Cai, and Y. Wang, *Nanoscale* **7**, 642 (2015).

³⁰Z. T. Xu, K. J. Jin, L. Gu, Y. L. Jin, C. Ge, C. Wang, H. Z. Guo, H. B. Lu, R. Q. Zhao, and G. Z. Yang, *Small* **8**, 1279 (2012).

³¹J. H. Stathis, *J. Appl. Phys.* **86**, 5757 (1999).